

**SMASIS2014-7481**

## **EXPERIMENTAL CHARACTERIZATION OF A CIRCULAR DIAPHRAGM DIELECTRIC ELASTOMER GENERATOR**

**Michele Righi**

**Rocco Vertechy**

**Marco Fontana**

PERCRO SEES, TeCIP Institute, Scuola Superiore Sant'Anna  
Piazza Martiri della Libertà 33, Pisa, 5612, Pisa, Italy  
E-mail: r.vertechy@sssup.it, m.fontana@sssup.it

### **ABSTRACT**

Inflated Circular Diaphragm Dielectric Elastomer Generators (CD-DEGs) are a special embodiment of polymeric transducer that can be used to convert pneumatic energy into high-voltage direct-current electricity. Potential application of CD-DEGs is as power take-off system for wave energy converters that are based on the oscillating water column principle. Optimal usage of CD-DEGs requires the adequate knowledge of their dynamic electro-mechanical response. This paper presents a test-rig for the experimental study of the dynamic response of CD-DEGs under different programmable electro-mechanical loading conditions. Experimental results acquired on the test-rig are also presented, which highlight the dynamic performances of CD-DEGs that are based on acrylic elastomer membranes and carbon conductive grease electrodes.

### **INTRODUCTION**

Dielectric Elastomer Generators (DEGs) are a very promising technology for the development of energy harvesting devices that rely on the variable-capacitance electrostatic generator principle [1, 2].

One of the most promising fields of application for DEGs is in the ocean energy sector [3-8], where they could be used to replace traditional Power Take Off (PTO) systems of Wave Energy Converters (WECs) that are based on conventional fluid and electromagnetic machinery.

Maximization of the energy that can be converted by a DEG-based WEC requires appropriate design and control methodologies, which make it possible to match the non-linear electro-elastic response of the DEG to the non-linear fluidodynamics of the WEC [5, 7, 8].

A very interesting concept of DEG-based WEC is the Polymeric Oscillating Water Column (Poly-OWC) [5, 7]. In Poly-OWCs, the pneumatic power generated by ocean waves in a semi-submerged air chamber is converted into high-voltage

direct-current electricity via an inflating Circular Diaphragm DEG (CD-DEG).

To date, the energy harvesting performance of CD-DEGs has been investigated via both numerical simulations [9] and practical experiments [10]. Theoretical studies have been aimed at assessing the influence of elastomer visco-elasticity on CD-DEG energy density and efficiency; they however neglected the influence of current leakage, which is a major cause of performance degradation in practical DEGs. Experimental studies investigated the electro-mechanical response and performance of a generic CD-DEG specimen for a single operating condition only.

In this context, this paper reports on the development of an experimental test-rig that has been predisposed for the study of CD-DEGs in dynamic regimes that are typical to those experienced in Poly-OWC systems. The test-rig comprises a CD-DEG, which includes driving and control electronics, and a cylindrical air chamber with actuated piston and pressure sensor, which makes it possible to accurately mimic OWC fluidodynamics. Preliminary experimental results acquired on the test-rig are also presented, which highlight the dynamic response and harvesting performance of a CD-DEG specimen for different sinusoidal motions of the piston and for different states of electrical activation of the CD-DEG.

### **EXPERIMENTAL SETUP**

The test-bench that has been developed for the experimental study of CD-DEGs is schematized in Figure 1. The test-bench comprises: a CD-DEG specimen; a mechanical sub-system; a high-voltage (HV) electronics sub-system; a real-time controller sub-system. Specific details of each sub-system are provided below.

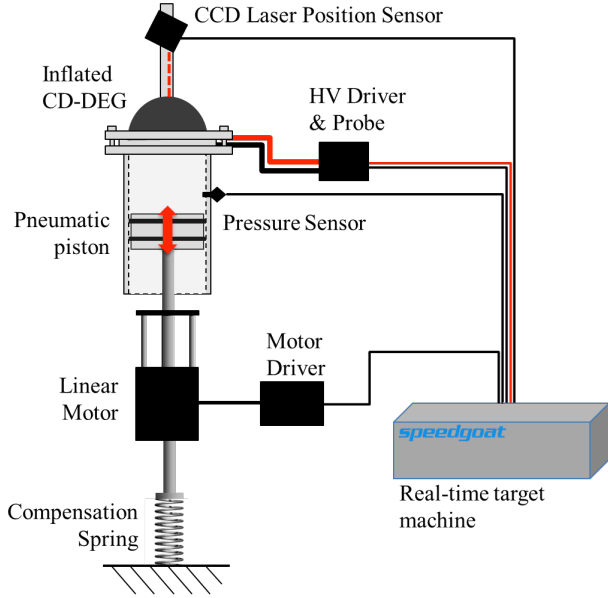


**Figure 1. Schematic of the experimental test-rig.**

*CD-DEG Specimen.* The CD-DEG considered for this study features the multi-stack architecture schematized in Figure 2. The specimen is made by an active dielectric elastomer membrane, which is obtained by gluing together three layers of a commercial double-sided pressure-sensitive acrylic tape (VHB 4905 by 3M<sup>®</sup>), that is stretched onto a polycarbonate ring and coated on both sides with compliant carbon conductive grease electrodes (MG-Chemicals 846). To prevent charge leakage through air, the HV electrode is encapsulated via an additional layer of acrylic tape (denoted as “leakage guard” in Figure 2), which is also stretched and glued along its perimeter to the polycarbonate ring.

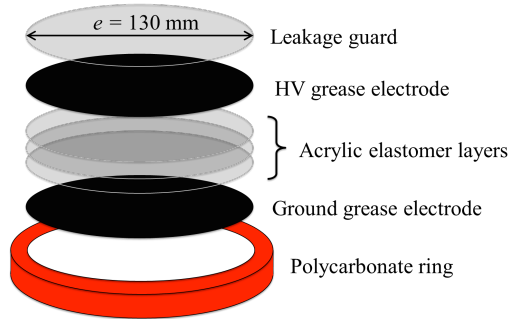


**Figure 2. Schematic of the CD-DEG assembly.**

The dimension of the internal diameter of the polycarbonate ring is  $e = 130\text{mm}$ ; acrylic film pre-stretch is equi-biaxial with value  $\lambda_p = 3.55$  (that is the same for both active dielectric elastomer membrane and leakage guard); the initial thickness (in the undeformed virgin condition) of the active dielectric elastomer membrane is  $t_0 = 1.5\text{mm}$ , which excludes the thickness of the compliant electrodes as well as that of the leakage guard (that is  $0.5\text{mm}$  in the undeformed virgin condition). Pictures of the CD-DEG prototype that has been

employed for this study are reported in Figure 3, with right and left images showing the specimen in its deflated and inflated states, respectively.

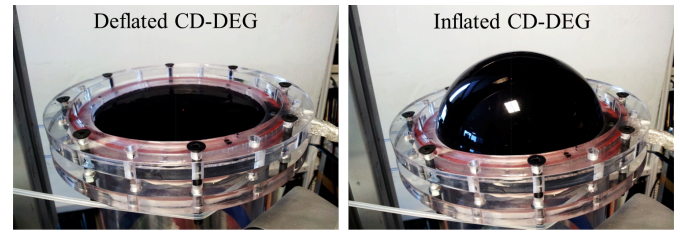


**Figure 3. CD-DEG prototype: deflated state (left), inflated state (right).**

*Mechanical Sub-system.* To simulate the Poly-OWC air chamber, a custom made pneumatic cylinder has been constructed that features: a polycarbonate cylinder tube (with internal diameter  $e = 130\text{mm}$ ); a movable piston; the CD-DEG specimen as upper end-cap. Air leakages are minimized by using a planar annular gasket with a tight screwed fixture on the CD-DEG side and appropriate pneumatic circular seals on the piston side. The piston is actuated via a brushless linear motor (P01-37x120F/200x280-HP by LinMot), with embedded encoder that is used to measure piston position,  $x$ . A pressure sensor (MPX12 by Freescale Semiconductor) installed on the cylinder tube is used to measure the differential pressure,  $p$ , between cylinder chamber and ambient air. A high-speed high-accuracy CCD laser displacement sensor (LK-G152 by Keyence), which is mounted on top of the cylinder head, is used in order to measure CD-DEG tip displacement,  $h$ . The pneumatic cylinder is mounted vertically and an elastic spring is introduced in order to compensate for the weight of both piston and motor slider.

*HV Electronics.* A custom made HV driving electronics has been developed to control CD-DEG charge and discharge. As depicted in Figure 4, the considered driving electronics comprises a HV power supply (10C24-P125 by UltraVolt) and two HV reed relays (HM12-1A69-150 by MEDER electronic) that alternatively connect the CD-DEG electrodes to either the power supply or to ground. In the circuit, resistor  $R_1$  ( $R_1 = 20\text{M}\Omega$ ) is used to fully discharge the power supply as the relay  $S_1$  is opened, whereas resistor  $R_2$  ( $R_2 = 1\text{M}\Omega$ ) is used to limit the peak current that occurs during CD-DEG discharge as the relay  $S_2$  is closed. To measure the electric potential difference,  $V$ , between CD-DEG electrodes, a custom made HV probe has been implemented that features very high input resistance (nearly  $50\text{G}\Omega$ ), which drastically limits the drain of charge from the CD-DEG electrodes, and large bandwidth, which is obtained thanks to a capacitor compensation network (see the high voltage probe schematic reported in Figure 4). In order to minimize the current leakage of the power electronics, all the HV wirings and components have been encapsulated via thick layers of silicone gel (Magic gel by Raytech) and acrylic tape (VHB 4905 by 3M<sup>®</sup>).

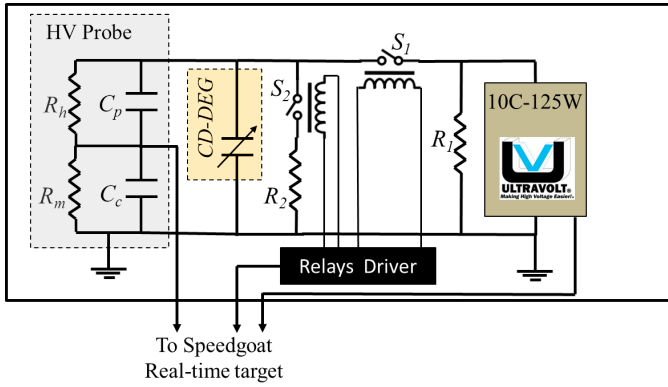
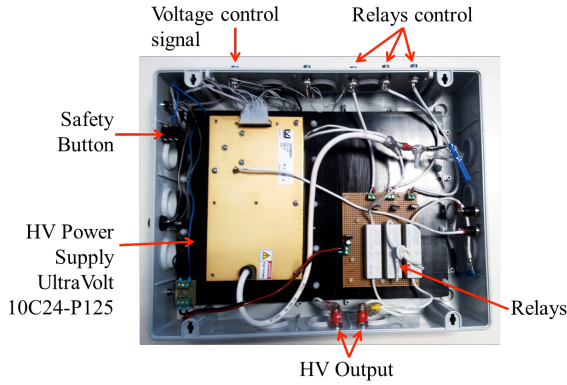


**Figure 4. Picture (top) and schematic (bottom) of the HV Driving circuit.**

**Controller.** A real-time machine (Performance real-time target machine by SpeedGoat<sup>®</sup>) running the MatLab<sup>®</sup> xPC Target<sup>®</sup> software environment is employed to control both the motion of the piston and the charging status (voltage) of the CD-DEG. This set-up enables to command any complex profile for piston position,  $x$ , and CD-DEG voltage,  $V$ , which can be generated via software on the basis of available measurements and properly defined dynamic models (for instance the model of OWC hydro-dynamics). For CD-DEG characterization purposes, in this work, the position of the piston is simply controlled according to programmed sinusoidal trajectories with different amplitudes,  $H$ , and frequencies,  $f$ , whereas CD-DEG voltage is controlled according to energy harvesting cycles at constant charge for different values of charging voltages,  $V_{in}$ . Specifically, the controller for the CD-DEG voltage relies on the measurement of the pressure,  $p$ , in the cylinder chamber, along with its time derivative, and runs according to the following sequence of operations:

- 1) instantaneously charge the CD-DEG, with a power supply voltage equaling  $V_{in}$ , when the diaphragm gets maximally expanded (that is, when the CD-DEG capacitance reaches a maximum value,  $C_{in}$ );
- 2) keep the CD-DEG disconnected as it returns to the flat configuration;
- 3) discharge the CD-DEG to ground when it reaches the flat configuration (that is, when the CD-DEG capacitance reaches its minimum value,  $C_{out}$ , and the electric potential

difference between the CD-DEG electrodes reaches a maximum value,  $V_{out}$ );

- 4) keep the charge zero as the CD-DEG expands.

Triggering between states 4 and 1 is obtained by monitoring the inversion of the time derivative of the pressure signal (in particular the condition  $[\dot{p} \leq 0 \text{ and } p \geq 0]$  when the CD-DEG is expanded outward and  $[\dot{p} \geq 0 \text{ and } p \leq 0]$  when the CD-DEG is expanded inward); triggering between states 2 and 3 is obtained by monitoring the inversion of the pressure signal (in particular the condition  $[\dot{p} \leq 0 \text{ and } p \leq 0]$  when the CD-DEG is expanded outward and  $[\dot{p} \geq 0 \text{ and } p \geq 0]$  when the CD-DEG is expanded inward); triggering between states 1 and 2 as well as between states 3 and 4 is obtained after a fixed time interval equaling 0.01s (that is enough to guarantee the complete charge and discharge of the CD-DEG in all the testing conditions).

## EXPERIMENTAL PROCEDURE

The test-bench described in the previous section has been employed for the dynamic characterization of a CD-DEG specimen. During the experiments, the electro-mechanical response of the considered CD-DEG has been evaluated for different sinusoidal motions (with different frequencies  $f$  and amplitudes  $H$ ) imposed on the pneumatic piston and for different charging voltages ( $V_{in}$ ) applied to the CD-DEG electrodes. Specifically, ten values for the charging voltages have been considered,  $V_{in} = [1.5\text{kV}, 2\text{kV}, 2.2\text{kV}, 2.4\text{kV}, 2.6\text{kV}, 2.8\text{kV}, 3\text{kV}, 3.2\text{kV}, 3.4\text{kV}, 3.6\text{kV}]$ ; three values for the piston motion amplitude have been considered,  $H = [15\text{mm}, 30\text{mm}, 45\text{mm}]$ ; four different values for the piston motion frequency have been considered,  $f = [0.6\text{Hz}, 0.8\text{Hz}, 1\text{Hz}, 1.2\text{Hz}]$ . Overall, 120 tests have been conducted on the same CD-DEG specimen.

For each test, piston motion was started from the same resting location and with the CD-DEG being in its flat configuration. In this starting condition, the volume of air that is entrapped between piston and CD-DEG was  $2\text{dm}^3$ . To guarantee the achievement of a stabilized response of the CD-DEG (with negligible remnant stress softening), a waiting time by about fifteen periods was respected prior to begin data acquisition and CD-DEG activation (i.e., energy harvesting). For simplicity, CD-DEG activation was performed only one time in a period; in particular during the cycle where the CD-DEG was expanding outward. For each acquisition, three-to-five periods with the CD-DEG inactive and eight-to-ten periods with the CD-DEG active were recorded. During experiments, piston displacement,  $x$ , CD-DEG voltage and tip height,  $V$  and  $h$ , and chamber pressure,  $p$ , measurements were acquired at 1kHz.

After completion of the test campaign, all the acquired data were post-processed to obtain: the evolution of the CD-DEG capacitance,  $C$ ; the energy harvested per cycle,  $E_{hc}$ ; the voltage amplification ratio,  $\phi$ ; the capture factor,  $\eta$ , from available mechanical energy to generated electricity; and the viscous loss,  $\zeta$ , that is mainly due to the visco-elasticity of the dielectric elastomer.

The evolution in time of the CD-DEG capacitance is computed as that of a planar circular capacitor with variable thickness [5], that is

$$C(h) = \frac{\pi \epsilon e^2 \lambda_p^2}{3t_0} \left[ \left( \frac{h^2 + e^2}{e^2} \right)^3 + \left( \frac{h^2 + e^2}{e^2} \right)^2 + \left( \frac{h^2 + e^2}{e^2} \right) \right], \quad (1)$$

where  $\epsilon$  is the dielectric constant of the considered DE material. Here  $\epsilon = 3.6 \cdot 8.8e^{-12}$  F/m has been selected based on capacitance measurements performed at  $h = 0$  via a LCR meter (Hameg Instruments HM 8118). Given Eq. (1), the electrical energy that is harvested in a cycle is computed as

$$E_{hc} = \frac{1}{2} [C_{out} V_{out}^2 - C_{in} V_{in}^2]. \quad (2)$$

The voltage ratio is computed as

$$\phi = V_{out} / V_{in}. \quad (3)$$

Given Eq. (2), the capture factor is calculated as

$$\eta = E_{hc} / E_m, \text{ with } E_m = \int_{T_1}^{T_2} W dt, \quad (4)$$

where  $T_1$  and  $T_2$  are two consecutive time instants, during the CD-DEG outward expansion, where the piston power,  $W$ ,

$$W = \frac{\pi e^2}{4} p \frac{dx}{dt}, \quad (5)$$

turns from negative to positive and from positive to negative, respectively.

The viscous loss is calculated as

$$\zeta = 0.5 E_d / E_m, \text{ with } E_d = \int_{T_1}^{T_1+1/f} W dt, \quad (6)$$

where  $E_d$  is the mechanical energy that is lost in a period, which is mainly due to CD-DEG viscoelasticity.

Worth to be remarked: 1)  $E_m$  and  $E_d$  also include the viscoelastic contribution of the leakage guard; 2)  $E_d$  is calculated over an entire period and by considering only the first cycles where the CD-DEG is kept inactive; 3) the calculation of  $\eta$  is performed by considering only the half cycle (in a period) in which the CD-DEG is expanded outward (evaluation over the entire period would have required the CD-DEG to be activated also in the half cycle in which it is expanded inward); 4) the calculated  $\eta$  neglects the electric losses that occur in passing the harvested energy from the CD-DEG electrodes to the external energy storage.

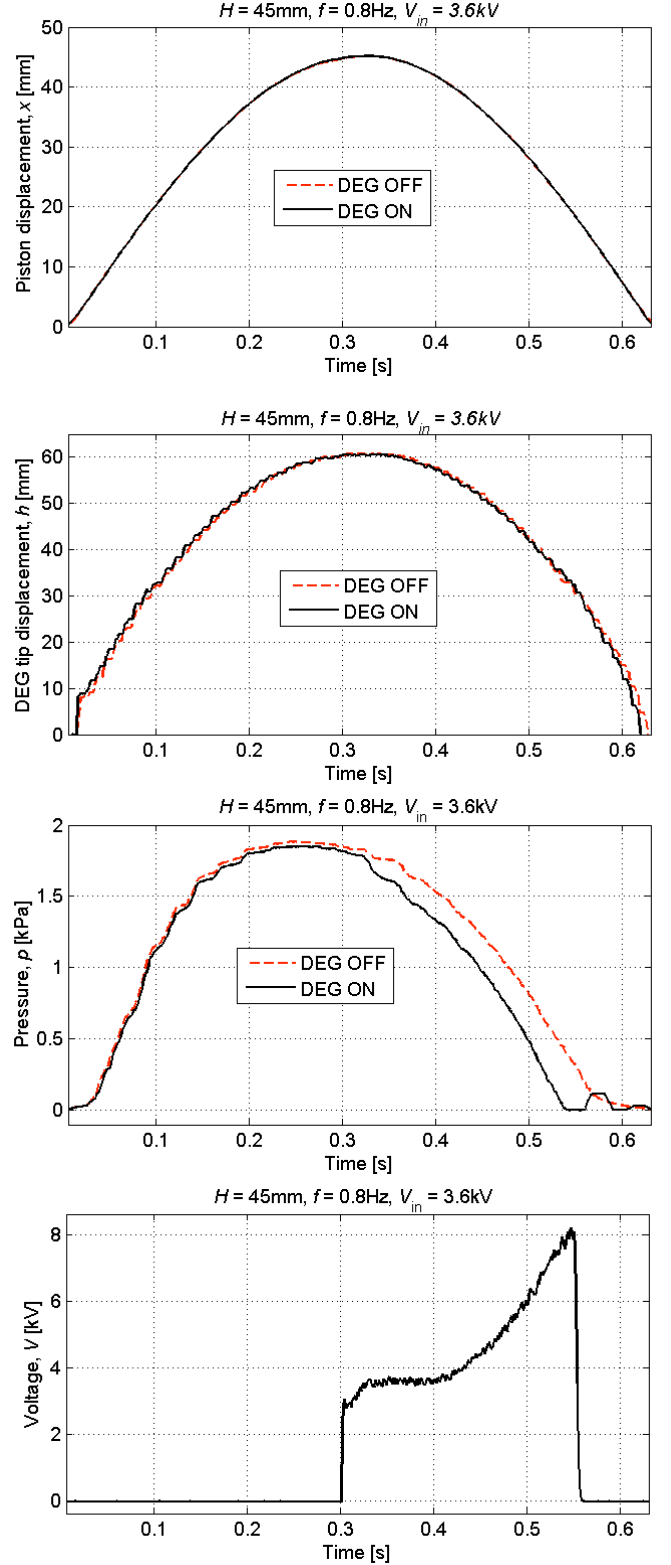


Figure 5. Experimental response of the CD-DEG for a sinusoidal motion of the piston with amplitude  $H = 45\text{mm}$  and frequency  $f = 0.8\text{Hz}$ , and for a charging voltage  $V_{in} = 3.6\text{kV}$ : motion of the piston; CD-DEG tip displacement; air chamber pressure; CD-DEG voltage.

## EXPERIMENTAL RESULTS

This section summarizes the results of the experimental campaign performed on the same CD-DEG specimen with the test-rig and procedures described above.

To provide an example of the measurements acquired during the experiments, Figure 5 reports the time evolution of motor position,  $x$ , CD-DEG tip height and voltage,  $h$  and  $V$ , and air chamber pressure,  $p$ , for the portion of the period where the CD-DEG is expanded outward. Plots are for the test conducted at  $f = 0.8\text{Hz}$ ,  $H = 45\text{mm}$  and  $V_{in} = 3.6\text{kV}$ . Since the response of the system is very repeatable, the reported plots span a single deformation/harvesting cycle of the CD-DEG only. For the sake of comparison, the plots for  $x$ ,  $h$  and  $p$  consider the response of the CD-DEG both in the presence (solid line) and in the absence (dashed line) of electrical activation. The voltage plot only refers to the case where the CD-DEG is active (namely, when it harvests energy) and highlights the effective increase in electric potential difference (from  $V_{in} = 3.6\text{kV}$  to  $V_{out} = 8.2\text{kV}$ ) that is experienced by the charges residing on the CD-DEG electrodes as the CD-DEG contracts in area. As shown, CD-DEG activation makes it possible to harvest energy (in this case the energy harvested in a cycle is  $E_{hc} = 103\text{mJ}$ ), and this induces a sensible modification in the dynamic response of the overall system (the major modification being in the pressure response).

The summary of the performances of the CD-DEG for different piston motions and for different charging voltages is reported in Figures 6-10. Overall, the following can be stated for the considered specimen and test conditions:

- 1)  $\phi$ ,  $E_{hc}$  and  $\eta$  increase monotonically as  $H$  increases;
- 2)  $\phi$ ,  $E_{hc}$  and  $\eta$  decrease monotonically as  $f$  increases;
- 3)  $\phi$  decreases monotonically as  $V_{in}$  increases;
- 4)  $E_{hc}$  and  $\eta$  increase monotonically as  $V_{in}$  increases, but a saturation effect occurs as the charging voltage gets larger;
- 5)  $\zeta$  increases monotonically as  $H$  and  $f$  increase, but is rather unaffected by variations of  $V_{in}$ .

Statement (1) is obvious. In fact, the larger is  $H$ , the larger are the deflection and the capacitance variation of the CD-DEG.

Statement (5) is also trivial, since larger values of  $H$  and  $f$  make the CD-DEG to deform at larger rates, which increase the visco-elastic losses that occur within the dielectric elastomer material as well as in the compliant electrodes.

Statement (2) can be understood by considering the loss of tension condition [2], which limits the harvesting performance of practical DEGs, especially when used at the highest deformation rates. In fact, the unloading stress-strain response of the employed dielectric elastomer material becomes softer as the deformation frequency is increased, which makes the loss of tension condition to occur at lower electric loadings.

Statement (3) is motivated by the existence of current leakage losses, which occur within the CD-DEG as well as across the other high-voltage components of the power electronics, and that are larger for larger electric potential differences applied between the electrodes of the CD-DEG.

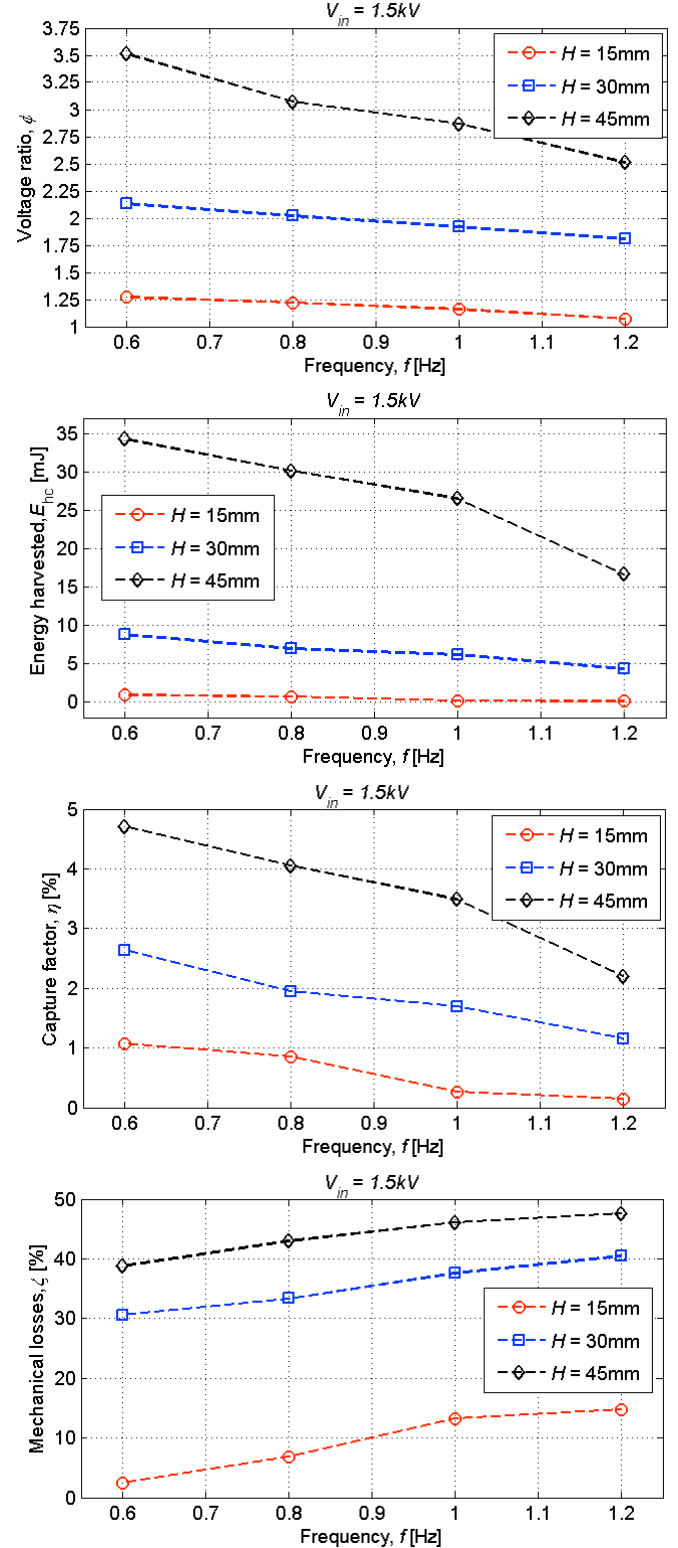


Figure 6. Experimental assessment of the CD-DEG for a sinusoidal motion of the piston: voltage amplification ratio, energy harvested per cycle, capture factor and mechanical loss as function of piston motion frequency,  $f$ , and amplitude,  $H$ . Results are for a CD-DEG charging voltage equaling  $V_{in} = 1.5\text{kV}$ .

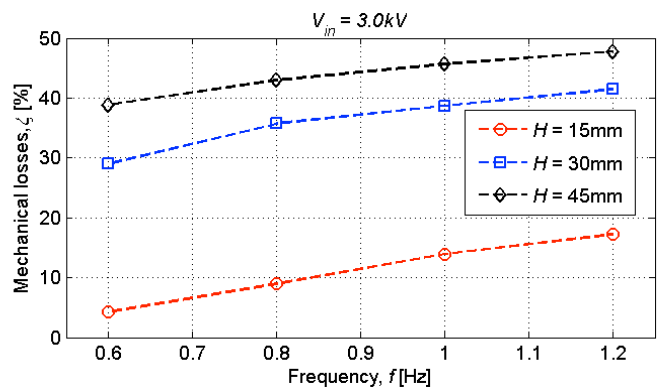
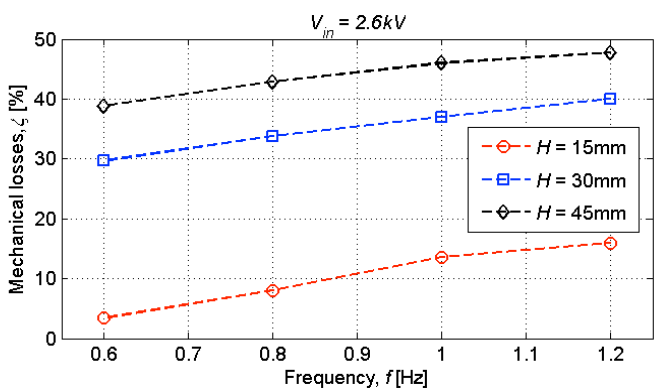
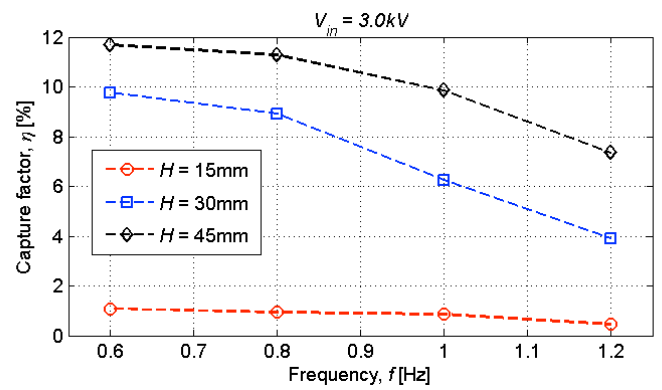
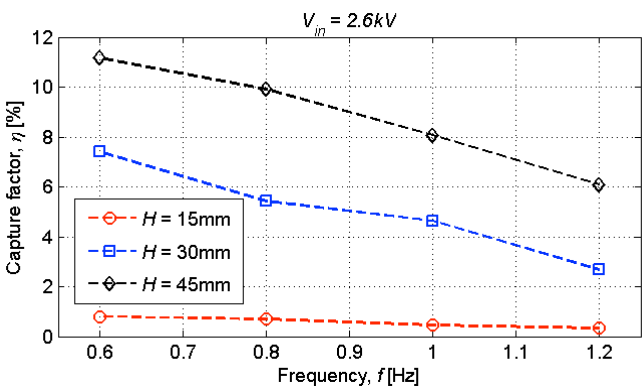
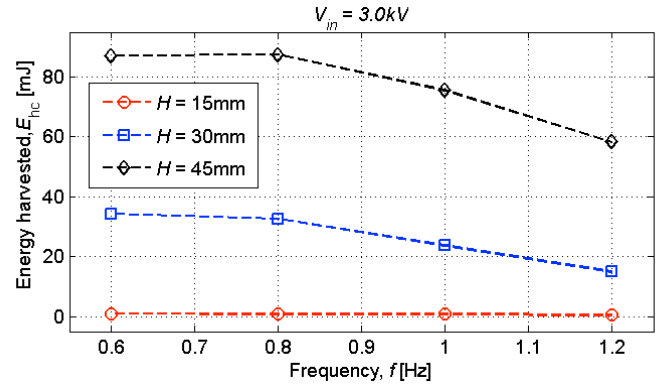
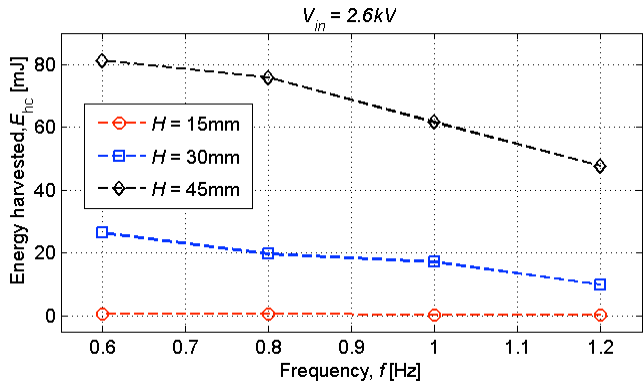
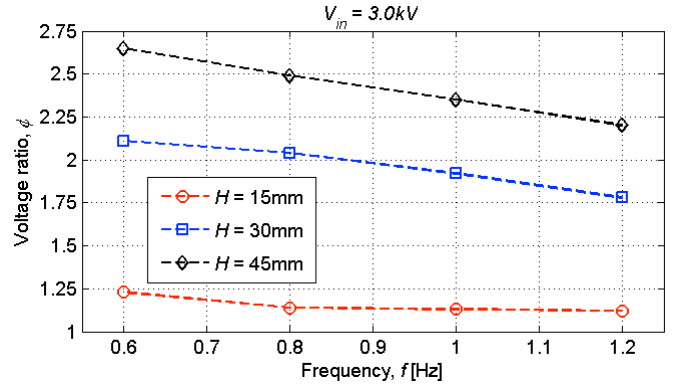
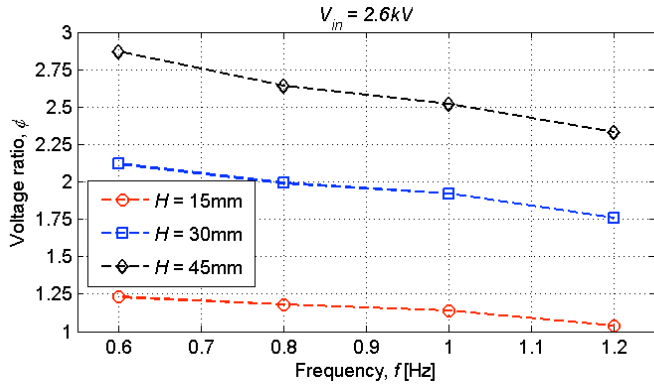


Figure 7. Experimental assessment of the CD-DEG for a sinusoidal motion of the piston: voltage amplification ratio, energy harvested per cycle, capture factor and mechanical loss as function of piston motion frequency,  $f$ , and amplitude,  $H$ . Results are for a CD-DEG charging voltage equaling  $V_{in} = 2.6kV$ .

Figure 8. Experimental assessment of the CD-DEG for a sinusoidal motion of the piston: voltage amplification ratio, energy harvested per cycle, capture factor and mechanical loss as function of piston motion frequency,  $f$ , and amplitude,  $H$ . Results are for a CD-DEG charging voltage equaling  $V_{in} = 3kV$ .

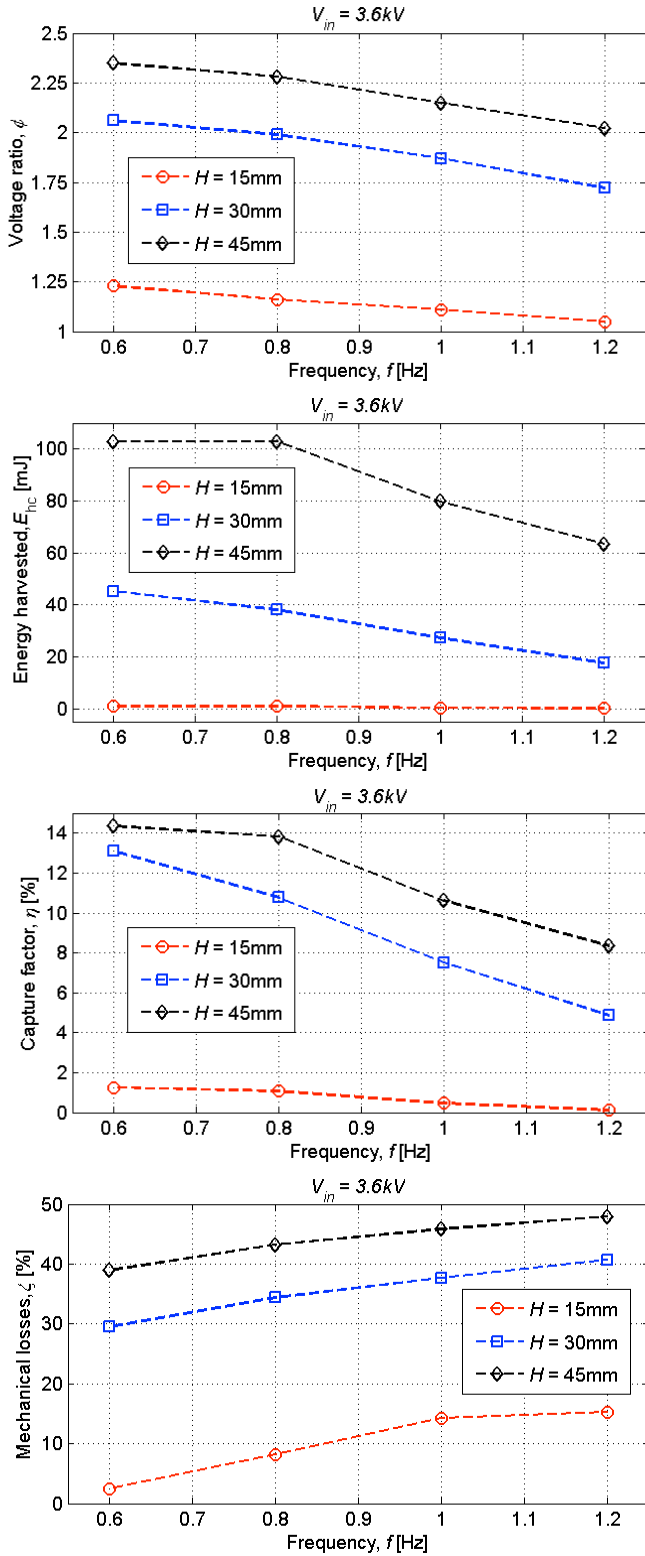


Figure 9. Experimental assessment of the CD-DEG for a sinusoidal motion of the piston: voltage amplification ratio, energy harvested per cycle, capture factor and mechanical loss as function of piston motion frequency,  $f$ , and amplitude,  $H$ . Results are for a CD-DEG charging voltage equaling  $V_{in} = 3.6 \text{ kV}$ .

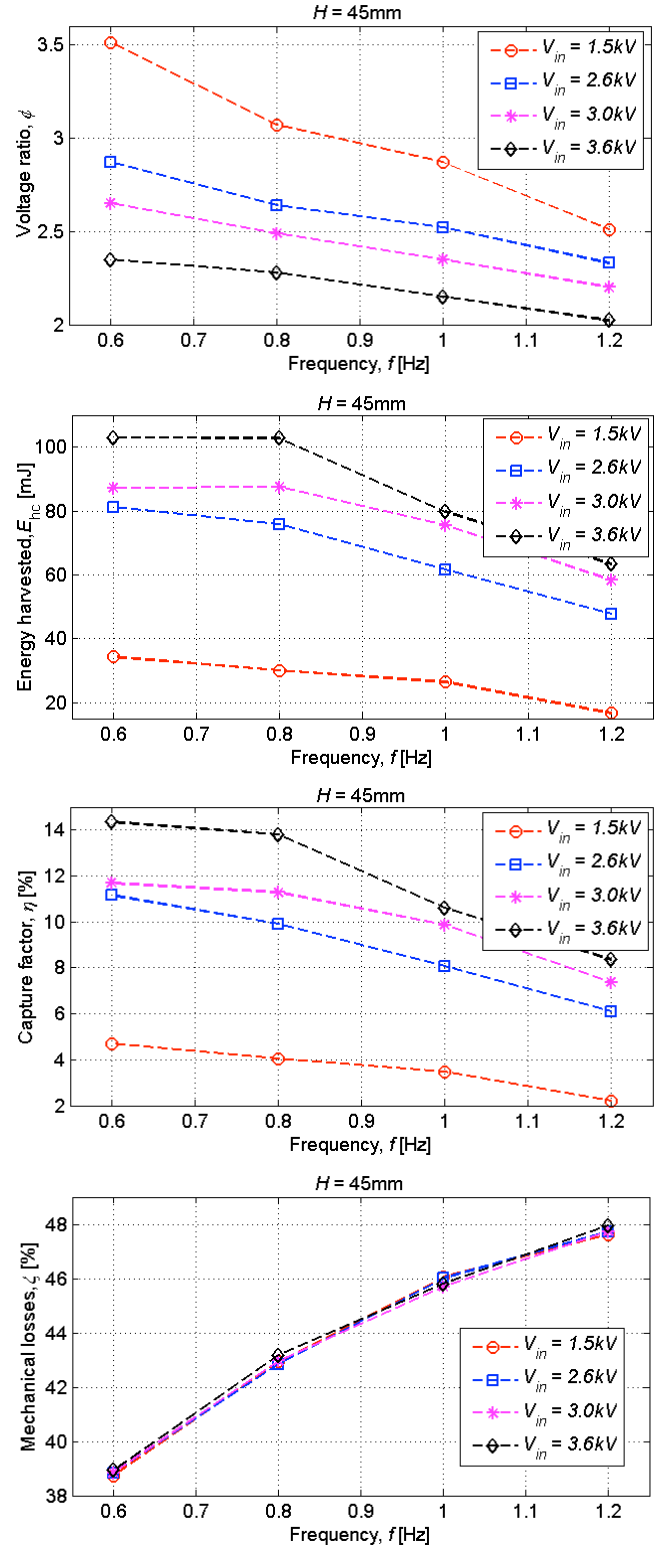


Figure 10. Experimental assessment of the CD-DEG for a sinusoidal motion of the piston: voltage amplification ratio, energy harvested per cycle, capture factor and mechanical loss as function of piston motion frequency,  $f$ , and CD-DEG charging voltage  $V_{in}$ . Results are for a piston motion amplitude equaling  $H = 45 \text{ mm}$ .

Statement (4) is motivated since the theoretical energy that can be converted by any CD-DEG is larger the larger is the charge that resides on its electrodes during the generation phase. The saturation effect that occurs at the largest charging voltages is related to the decrease in voltage ratio (thus, it is due to current leakage losses) that has been described above.

As regards maximal performance, the highest amount of energy that was harvested by the CD-DEG during the experimental campaign has been about 103mJ per cycle, whereas the highest capture factor has been about 14% (this number becomes higher if one neglects the viscoelastic contribution of the leakage guard). These maximum values occurred for a charging voltage  $V_{in} = 3.6\text{kV}$ , for a piston motion amplitude  $H = 45\text{mm}$  and for a piston motion frequency ranging in between  $f = 0.6\text{Hz}$  and  $f = 0.8\text{Hz}$ . Since the mass of the considered CD-DEG is roughly equal to 1.5g, the maximal energy density obtained during the experiments has been roughly equal to 68J/kg. This number is significantly smaller than the theoretical maximum (1.7 kJ/kg [2]) that is estimated for DEGs employing the same material and undergoing energy harvesting cycles with uniform equibiaxial deformations and controlled at maximum electric field. Major motivations for the reduced energy density exhibited during the experiments by the CD-DEG specimen are: 1) the deformation states undergone by the CD-DEG are neither uniform nor equi-biaxial; 2) the energy harvesting cycle is performed at constant charge rather than at maximum electric field; 3) the maximum electric field acting across the CD-DEG has been limited below  $75\text{MVm}^{-1}$  (rather than up to  $200\text{MVm}^{-1}$  as in [2]); 4) the theoretical maximum is evaluated for ideal conditions, thereby neglecting the negative effects of current leakage and visco-elasticity.

Beside making the loss of tension condition more severe, the intrinsic visco-elasticity of the employed dielectric elastomer also causes significant mechanical dissipations that, for the larger CD-DEG tip displacements, can waste a significant portion (in the range between 40% and 50%) of the mechanical energy that could be otherwise available for energy conversion.

## CONCLUSIONS

This paper presented an experimental test-rig for the study of the dynamic response of inflated Circular Diaphragm Dielectric Elastomer Generators (CD-DEGs). The test-rig makes it possible to characterize CD-DEGs under varying electro-mechanical loading conditions, as well as to perform hardware-in-the-loop simulations for the development and assessment of CD-DEGs, including their energy harvesting controllers, for specific applications.

Experimental results have also been provided to show the dynamic response and energy harvesting performance of a particular CD-DEG specimen, which is based on acrylic elastomer membranes and carbon conductive grease electrodes, over a wide range of electro-mechanical loading conditions.

In the future, hardware-in-the-loop simulations will be performed via the developed test-rig to optimize and assess CD-DEG power take-off systems for wave energy converters that are based on the oscillating water column principle.

## ACKNOWLEDGMENTS

The work presented in this paper is developed in the context of the project PolyWEC ([www.polywec.org](http://www.polywec.org)), a FP7 FET- Energy project. The research leading to these results has received funding from the European Union Seventh Framework Programme [FP7/2007-2013] under grant agreement n° 309139.

## REFERENCES

- [1] Pelrine, R., Kornbluh, R., Eckerle, J., Jeuck, P., Oh, S., Pei, Q., Stanford, S., 2001. "Dielectric elastomers: Generator mode fundamentals and applications". In Proceedings of SPIE Vol. 4329, pp. 148-156.
- [2] Koh, S.J.A., Keplinger, C., Li, T., Bauer, S., Suo, Z., 2011 "Dielectric elastomer generators: How much energy can be converted?", IEEE/ASME Transactions on Mechatronics, 16(1), 33-41.
- [3] Chiba, S., Waki, M., Kornbluh, R., Pelrine, R., 2008. "Innovative power generators for energy harvesting using electroactive polymer artificial muscles". In Proceedings of SPIE 6927, pp. 692715.
- [4] Jean, P., Watez, A., Ardoise, G., Melis, C., Van Kessel, R., Fourmon, A., Barrabino, E., Heemskerk, J.; Queau, J.P., 2012. "Standing wave tube electro active polymer wave energy converter". In Proceedings of SPIE 8340, pp. 83400C.
- [5] Rosati Papini, G. P., Vertechy, R., Fontana, M., 2013. "Dynamic Model Of Dielectric Elastomer Diaphragm Generators For Oscillating Water Column Wave Energy Converters". In Proceedings of ASME 2013 Conference on Smart Materials, Adaptive Structures and Intelligent Systems, Snowbird, Sept. 16–18, doi:10.1115/SMASIS2013-3255.
- [6] Scherber, B., Grauer, M., Köllnberger, A., 2013. "Electroactive polymers for gaining sea power". In Proceedings of SPIE Vol. 8687, pp. 86870K.
- [7] Vertechy, R., Fontana, M., Rosati Papini, G.P., Forehand, D., 2014. "In-tank tests of a dielectric elastomer generator for wave energy harvesting". In Proceedings of SPIE Vol. 9056, pp. 90561G.
- [8] Moretti, G., Forehand D., Vertechy R., Fontana M., Ingram D., 2014. "Modeling of an oscillating wave surge converter with dielectric elastomer power take-off". In Proceedings of ASME 2014 33rd International Conference on Ocean, Offshore and Arctic Engineering, San Francisco, CA, USA, 8-13 June, Paper No. OMAE2014-23559.
- [9] Li, T., Qu, S., Yang, W., 2012. "Energy harvesting of dielectric elastomer generators concerning inhomogeneous fields and viscoelastic deformation", Journal of Applied Physics, vol. 112, pp. 034119.
- [10] Kaltseis R., Keplinger C., Baumgartner R., Kaltenbrunner M., Li T., Mächler P., Bauer, S. (2011). Method for measuring energy generation and efficiency of dielectric elastomer generators. Applied Physics Letters, vol. 99, pp. 162904.